Presented at the 28th European PV Solar Energy Conference and Exhibition, 30 September - 4 October 2013, Paris, France

LASER DOPING FROM BOROSILICATE GLASS FOR METALLIZATION OF BORON EMITTERS

S. Fernandez-Robledo, U. Jäger, E. Lohmüller, J. Nekarda
Fraunhofer Institute for Solar Energy Systems
Heidenhofstrasse 2, 79110 Freiburg im Breisgau, Germany
Phone: +49 (0) 761/4588-5057; Fax: +49 (0) 761/4588-781
e-mail: Susana.Fernandez.Robledo@ise.fraunhofer.de

ABSTRACT: The improvement of the contact resistance with the modification of the dopant profile is investigated for n-type solar cells. Metallization was performed by screen printing. The dopant profile is controlled by laser doping. Different powers of a laser with a wavelength of $\lambda = 355$ nm and a pulse length of $\tau_{Laser} \approx 25$ ns were tested. Laser doping was carried out on two emitters ($R_{sheet} \approx 70$ and 90 Ω/sq.) and their corresponding borosilicate glass (BSG) precursor layers, which were grown with the emitter during tube furnace diffusion. Only a small part of the boron is diffused from the BSG layer into the silicon. This is explained by the low heat diffusion in the BSG layer, since it was found that the surface dopant concentration diffused into silicon increases after laser doping with higher laser powers. The boron profiles obtained by laser doping presents lower surface concentration but deeper dopant profiles than the emitters without laser doping. The emitter saturation current density results indicate that the recombination increases strongly for laser doping samples. Specific contact resistances were reduced half for laser doping samples in comparison to the homogeneous tube furnace diffused emitters, reaching a minimum value of 5.2±1.2 mΩ·cm^2.

Keywords: boron, n-type, laser doping, selective emitter, diffusion, contact

1 INTRODUCTION

n-type silicon material is very attractive compared to p-type for the photovoltaic industry, due to its higher tolerance to common impurities [1], hence higher minority carriers lifetimes, and no degradation by formation of boron-oxygen complexes by light-induced degradation (LID) [2, 3]. The advantages of using n-type material have motivated a growing research effort for adapting the solar cell manufacturing from p-type to n-type substrates.

A homogeneous p+ emitter can be created in n-type silicon by BBr_3 tube furnace diffusion. Low surface doping concentration emitters are desired for high efficiency solar cells, so the losses due to minority carrier recombination are minimized, higher open circuit voltages and solar cell efficiencies are reached. However, their metal contact resistance and lateral conductivity are higher than for high surface doping concentration emitters.

On p-type emitters, one well known approach to solve this problem is to overdope by laser the regions under the metal contacts using selective emitter [4-6]. This heavy doping below the contacts behaves as a barrier that prevents the minority carrier flowing into the front contacts, and therefore reduces their recombination.

Selective emitter can be formed easily by laser doping, since it is possible to choose the dopant precursor layer and the suitable laser parameters. Laser flexibility allows adapting the doping profiles characteristics, such as surface concentration and depth, to the particular requirements of the desired metallization approach. The laser heats the silicon and the dopant precursor layer only where is necessary, to increase the dopant diffusion coefficient when silicon and precursor layer are melted. Besides, masks are not required, which reduces the number of steps for solar cell manufacturing.

In this work, it is investigated how laser doping can contribute to the improvement of the specific contact resistance of n-type base solar cells for screen printing metallization. Laser doping is performed on borosilicate glass (BSG) precursor layers, i.e silicon oxide layers doped with boron. This can be a cost effective process, since the layer grows during the diffusion of the homogeneous boron emitter.

Different laser processes were tested, by means of laser power variation, to obtain different surface concentrations and depths of diffused dopant in the emitter. The specific contact resistance is measured for these laser processes. Characterization of the precursor layer, doping diffused into silicon concentration and emitter saturation current density is carried out to understand better the results from the specific contact resistance measurements.

2 EXPERIMENTAL DETAILS

The optimum laser doping process to achieve a good specific contact resistance is investigated by determining the dopant concentration and optical properties of the precursor layer, the dopant profiles of boron (B) diffused in silicon (Si), the emitter saturation current density (J_{0e}) and the specific contact resistance (ρ_c). A process flow of this experiment is presented in Figure 1.

The wafers used were 125x125 mm^2 n-type FZ-Si wafers with saw damage-etched (SDE) and alkaline textured (TEXT) surfaces, and Cz-Si wafers with textured front side and SDE on the rear side.

Two p+ emitters (BSG-70 and BSG-90 emitter) were tested. Both of them were fabricated by BBr_3 tube furnace diffusion and have a surface doping concentration of around 1x10^{20} cm^{-3}. The BSG-90 emitter has a depth of ≈ 0.5 µm ($R_{sheet} \approx 90$ Ω/sq.), while the BSG-70 emitter was diffused at higher temperature and reaches a depth of ≈ 0.7 µm ($R_{sheet} \approx 70$ Ω/sq.).

Laser doping was carried out with a frequency tripled Nd:YVO_4 DPSSL, a Coherent AVIA 355X, at a

wavelength of $\lambda = 355$nm and a pulse length of approximately $\tau_{Laser} = 25$ ns. Full doping areas were made by overlapping laser doping lines. For the Quasi-steady-state photo-conductance (QSSPC) samples, laser doping was performed symmetrically (on both sides of the wafer) for J_{0e} determination. For the by transmission line method (TLM) [7-10] samples, laser doping was performed on the textured side of the Cz wafers, over full doped areas.

After laser doping, the remaining BSG was etched off with hydrofluoric acid (HF).

Passivation and antireflection coating layers were fabricated by deposition of AlO_x and SiN_x symmetrically (on both sides of the wafers) for J_{0e} samples. TLM structures were prepared by metallization of the laser doping areas with screen printed 90 µm thick finger contacts using a commercial available silver-aluminum paste. QSSPC and TLM samples were fired at 800°C in an industrial inline fast firing furnace, so the passivation is activated and the metal penetrates through the passivation layer forming the electrical conductive contact. TLM samples were cut with a dice saw machine before measurements, to prevent lateral current flow.

Precursor layer characterization was carried out by means of inductively coupled plasma mass spectrometry (ICP-MS), X-ray photoelectron (XPS).

The laser doping process was characterized measuring sheet resistances (R_{sheet}) by Four Point Probe, the dopant profiles by Electrochemical Capacitance Voltage (ECV) [11] tool CVP21 from WEP, the effective lifetime by QSSPC measurements to extract J_{0e} using a Sinton Instruments WCT-120, and ρ_c by TLM measurements.

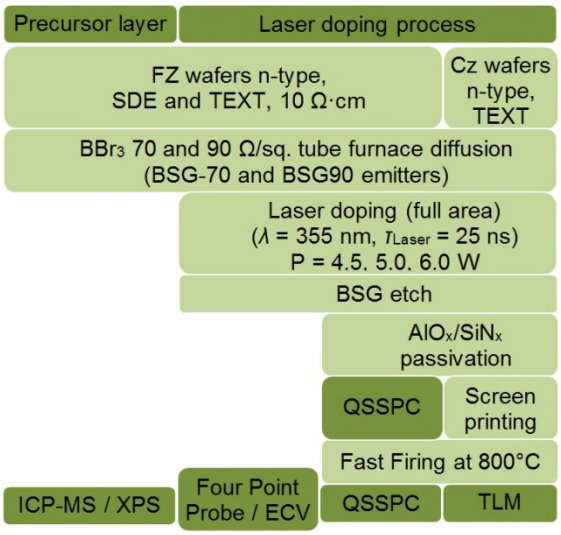

Figure 1: Process work flow of the experiment.

3 RESULTS AND DISCUSSION

3.1 Precursor layer of dopants

The dopant precursor layer for the 70 Ω/sq. emitter (BSG-70) was grown at a higher temperature than the precursor layer for the 90 Ω/sq. emitter (BSG-90), but for the same duration. The deposition rate and the diffusion of B in the Si are exponentially dependent on temperature and the activation energy, following the Arrhenius equation. This means that the deposition rate of the layer and the diffusion of B in Si will be faster for the BSG-70. Therefore, it is expected to find a higher concentration of B in the BSG layer of the BSG-70 process compared to BSG-90 diffusion. This is in agreement with the ICP-MS measurement results. The integrated B concentration, which does not depend on the thickness of the BSG layer, is shown in Table I.

Table I: Boron concentration and thickness of precursor layers and sheet resistance of the corresponding emitter.

Precursor Layer	**B conc.** (10^{16} cm^{-2})	**Thickness** (nm)	R_{sheet} **emitter** (Ω/sq.)
BSG-70	1.70±0.19	27.3±5.0	72.8±0.2
BSG-90	1.23±0.12	24.0±5.0	90.2±1.0

The diffusion of dopant from the precursor layer into Si by a laser doping process depends on the dopant concentration in the precursor layer, as well as on the optical properties of the precursor layers, such as the absorption and the reflection of the precursor layer at the laser wavelength. These parameters change with the thickness of the precursor layer. In this case, the thickness is similar for both precursor layers (see Table I). The absorption of the precursor layer is very low for UV wavelengths [12]. Hence, the heating of the precursor layer by absorption of laser radiation is not possible. Besides, thermal conductivity of BSG is quite low (1.2 Wm^{-1}K^{-1} while it is 37 Wm^{-1}K^{-1} for Si [13]) and the time of application of the heating source is very short ($\tau_{Laser} = 25$ ns). This can result in a smaller diffusion coefficient for B in SiOx, since diffusion coefficient increases strongly with temperature [14].

An XPS profile was measured for BSG-70 precursor layer (see Figure 2), obtaining a B concentration of 5.0%, 65.3% of oxygen and 29.7% of Si. There is a region with approximately a thickness of 10 nm in the Si/SiOx interface, where oxygen and silicon were measured, but no boron. This could act as a diffusion barrier, due to the segregation of B to the oxide.

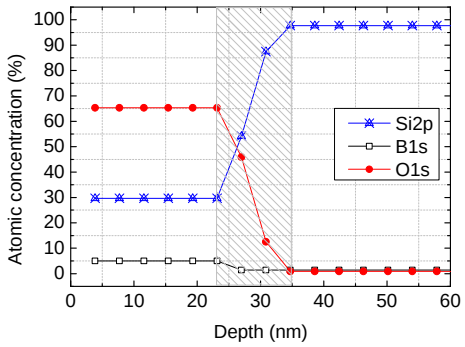

Figure 2: Boron, oxygen and silicon concentrations with depth for the precursor layer BSG-70 by XPS.

3.2 Doping concentration in silicon

During laser doping, the laser heats the Si and precursor layer locally, leading to diffusion of the dopant from the precursor layer and redistribution of dopant into the Si. When the silicon is melted, the dopant diffusion coefficient is increased [15]. The depth of the dopant diffused into the Si is increased with the laser power, since

higher laser powers lead to deeper Si melting depths [16]. However, the surface doping concentration decreases during such dopant redistribution, because there is not enough dopant from the precursor layer that is able to incorporate in the Si surface before reaching the equilibrium (diffusion from a limited source). Dopant diffusion in the Si surface during laser doping depends on the dopant concentration in the precursor layer, on the dopant segregation at Si/BSG interface and of the dopant diffusion coefficient in SiO_x and Si. The segregation coefficient of B at the Si/SiO_x interface is approximately 0.3 at equilibrium, compared to 10 for phosphorous [17]. This means that B dopants prefer to segregate to the oxide, that could leads to a depletion of B at the Si surface, while phosphorous tends to diffuse into the silicon and accumulates at the Si/SiO_x interface. Moreover, dopant diffusion can be decreased due to the difficulty for heating the BSG layer, and therefore to the lower diffusion coefficient (see section 3.1). Therefore, the amount of B from BSG films diffused in Si by laser doping is expected to be low compared to the amount of B available in the BSG layer.

The amount of dopant is related to the R_{sheet} through the following equation:

$$\boldsymbol{R_{sheet}} = \int_0^W \frac{dz}{e\mu_n(N,z)N(z)} \qquad (1)$$

where e is the elementary charge, μ_n the minority carrier mobility, W the junction depth and N the impurity density in the emitter region. Therefore, dopant concentration is higher for lower R_{sheet} values.

The variation of R_{sheet} with laser power is shown in Figure 3. R_{sheet} decreases with laser power, due to further dopant diffusion from the precursor layer into Si, or by deepen of the dopant profile (see Equation 1). A minimum $R_{sheet} \approx 40$ Ω/sq. is reached for all the samples at high laser powers.

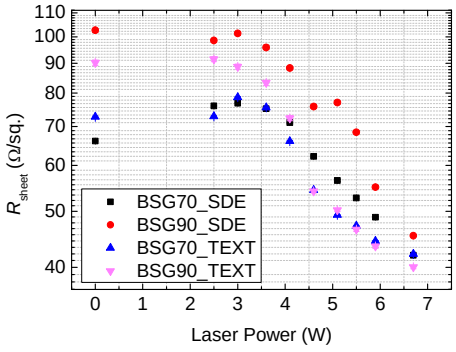

Figure 3: Sheet resistances variation with the laser doping power.

B dopant profiles of the laser doping on BSG-70 and BSG-90 samples are plotted for several laser powers in Figure 4. Dopant surface concentration decreases with power, while doping depth increases.

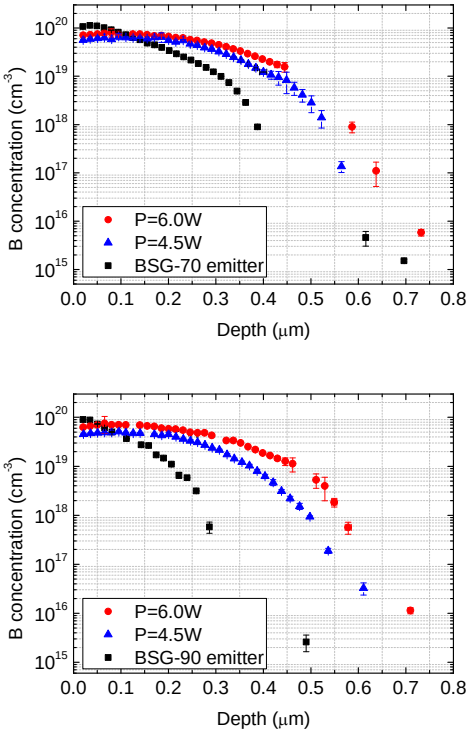

Figure 4: B concentration with depth measured by ECV for 70 Ω/sq. emitter (up) and for 90 Ω/sq. emitter (down).

B surface concentration is slightly higher for laser doping from BSG-70 than for BSG-90 precursor layer, which is related to a higher concentration of B in BSG-70 (see Table I). Surface dopant concentration is reduced by laser doping (BSG behaves as diffusion limited source). However, it increases with laser doping power (see Figure 4). When laser power is increased, the Si melting gets deeper and the time required for cooling is longer. Therefore the amount of heat energy available to be diffused from the Si to the precursor layer is higher.

After laser doping, the BSG layer remains with the same thickness than after layer deposition. This can be observed in the SEM images (see Figure 5), which were taken for the BSG-70 precursor layer irradiated with a laser powers of 2.5 W and 5.0 W.

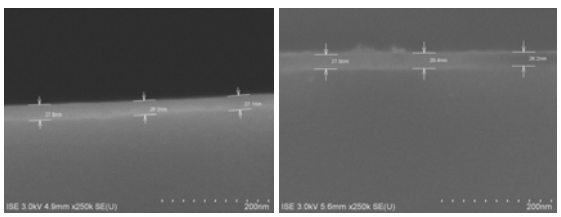

Figure 5: SEM images for BSG-70 after laser doping at 2.5 W (left) and 5.0 W (right). Thicknesses of 27.0±5.0 and 27.5±5.0 nm were measured before and after laser doping, respectively.

In order to determine if dopant from the precursor layer is incorporated into the Si by laser doping or if only occurs a redistribution of the already diffused B in the Si, the total amount of B incorporated was calculated by

integration of the ECV doping profiles. In this way, the doping concentration in cm^{-2} is obtained for each precursor layer and laser power. This integrated B concentration does not depend on the depth of the dopant diffused into the Si. The results are shown in Figure 6. B concentration in Si increases with power for laser doping from precursor layers BSG-70 and BSG-90.

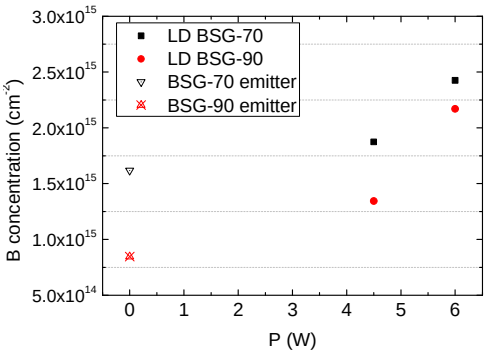

Figure 6: B concentration, obtained by integration of the ECV doping profiles, as function of laser power.

The maximum incorporation of B into Si was only approximately 10% of the B contained in the precursor layer.

3.3 Recombination in the emitter

The quality of an emitter can be evaluated by measuring J_{0e}. Highly doped volumes are a source of recombination which results in a reduction of the open circuit voltage, and therefore of the efficiency of the solar cell. In the case of diffusion of dopants by laser irradiation, extra sources of recombination could take place when the laser parameters and/or dopant precursor layer are not suitable. Some undesired impurities can be diffused from the precursor layer and/or the process atmosphere, as for example oxygen [18], nitrogen or carbon [19]. Besides, damage can appears in the surface and in the volume where laser irradiation is absorbed due to the fast cooling of the melted Si, with no time enough for a proper crystalline reorganization. Such damage introduces levels in the energy gap that leads to Shockley-Read-hall recombination. The rate of Auger recombination is also increased with the additional dopant that is diffused into the Si. As consequence of these recombination sources, J_{0e} is expected to be higher for laser doped volumes.

In order to determine the effect on J_{0e} of the different laser powers and the optimum laser doping process, J_{0e} was extracted from QSSPC measurements for the laser heavily-doped emitter regions for different laser powers. Measurements were performed at high injection level ($\Delta n >> N_D$, with Δn the excess carrier concentration and N_D the base doping concentration), where the J_{0e} is the dominating effect compared to τ_{bulk} (lifetime of the base), due to the low doping of the base. J_{0e} was extracted using the method explained by Kane and Swanson [20] with the parameterization from Kerr and Cuevas for the bulk Auger lifetime [21].

Laser doping was performed at laser powers of 6.0, 5.0 and 4.5 W. J_{0e} is plotted as function of R_{sheet} for each emitter and sample surface in Figure 7. J_{0e} increases strongly for laser doped samples compared to not laser doped samples. However, the J_{0e} increase is small when R_{sheet} decreases for the SDE samples, and not noticeable for the textured samples. Similar J_{0e} values were obtained for different R_{sheet} values in the case of SDE samples.

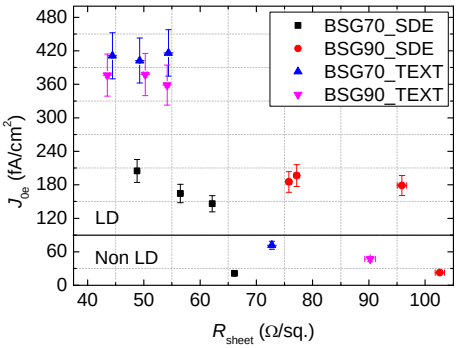

Figure 7: Emitter saturation current density as function of the sheet resistance for the two emitters in SDE and textured wafers after firing.

J_{0e} is almost double for textured wafers than for SDE wafers. This is related to the larger area of the textured surface, compared to the flat SDE surface samples. The increase of the effective surface can be corrected with a factor 1.7 [22]. Similar J_{0e} values are obtained for SDE and textured surfaces when this correction is performed.

J_{0e} decreases up to more than 8 times for the samples that were not irradiated by laser and only between 2 and 3 times for laser doping samples, when J_{0e} values before and after firing are compared. Hence, the passivation is more effective for the samples without laser doping. This means that the surface recombination is higher and/or the recombination that was introduced in the laser treated volume is too deep to be passivated by means of AlO_x/SiN_x surface passivation for the laser doping samples. An increase in the H content in the SiN_x could help in a further reduction from J_{0e} for the laser.

3.4 Specific contact resistance

Selective laser doping under metal electrodes can help to reduce the resistive losses in a solar cell. These losses can originate from high series resistance and shunts (low shunt resistances). Shunts can be prevented by choosing a laser diffusion process to get deeper dopant diffusion, which should cover the interface between metal and emitter and prevent the metal from spiking through the emitter. Series resistance of the emitter can be decreased by using a laser selective emitter, increasing the dopant concentration in the contact surface between the metal and emitter, and therefore reducing the contact resistance. In this section, it is evaluated how the specific contact resistance changes with several laser doping processes (laser powers).

The calculated specific contact resistances (ρ_c) are plotted as function of the R_{sheet} values measured by TLM in Figure 8. ρ_c decreases with decreasing R_{sheet}, and therefore it decreases with the dopant concentration under the metal contacts. After laser doping, the surface dopant concentration is lowered while the dopant diffusion depth is increased. Laser doped boron emitters from BSG feature a lower dopant surface concentration but deeper dopant profiles, and as result smaller R_{sheet} values. The importance of the depth of the B dopant profiles for contact formation has been also reported in reference [23].

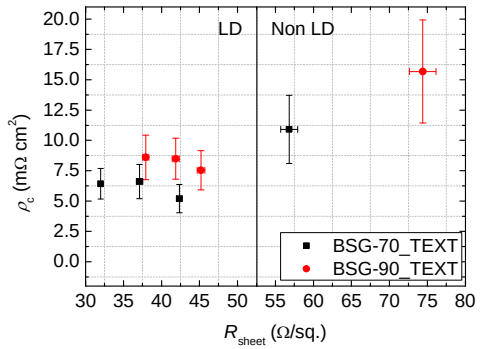

Figure 8: Specific contact resistance as function of sheet resistance measured by TLM for BSG-70 and BSG-90 with and without laser doping (LD).

ρ_c is reduced to half value when laser doping is performed (from 10.9±2.82 mΩ·cm^2 to 5.2±1.2 mΩ·cm^2 for BSG-70 and from 15.7±4.25 mΩ·cm^2 to 7.54±1.62 mΩ·cm^2 for BSG-90). The reduction of the contact resistance is more noticeable for high R_{sheet} (low dopant concentration, and therefore high contact resistances).

4 CONCLUSIONS

The specific contact resistances on n-type wafers for two boron emitters ($R_{sheet} \approx 70$ and ≈ 90 Ω/sq.) were reduced for a commercial screen printing paste by laser doping.

Laser doping was performed through the BSG layers for both tube furnace diffused emitters. The boron profiles obtained by laser doping presents lower surface concentration but deeper dopant profiles than the emitters without laser doping. $R_{sheet} \approx 40$ Ω/sq. were reached. When laser power is increased, the melting depth in silicon goes deeper, and there will be more heat available to diffuse to the precursor layer. This could explain the increase in dopant surface concentration with laser power observed in the dopant profiles. Laser doping efficiency increases for high laser powers.

The emitter saturation current density was measured for evaluating the recombination introduced for the laser doping. It was shown that it increases strongly for laser doping samples, where passivation is not so effective as for not laser doped samples.

Specific contact resistances were reduced half for laser doping samples in comparison to the homogeneous tube furnace diffused emitters, reaching a minimum value of 5.2±1.2 mΩ·cm^2.

5 ACKNOWLEDMENTS

The authors would like to thank A. Leimenstoll, F. Schätzle, N. Kohn, N. Hoffmann, S. Kühnhold, R. Neubauer and M. Retzlaff for processing, J. Zielonka, S. Schmutzler, A. Hartmann, M. S. Hendrichs, M. Linke and K. Mewes for measurements, and P. Saint-Cast, J. Benick and A. M. Moldovan for helpful discussions.

This work was supported by the German Federal Ministry for the Environment, Nature Conservation and Nuclear Safety within the research project "THESSO" under contract number 0325491.

6 REFERENCES

[1] D. Macdonald, L.J. Geerligs, Applied Physics Letters 85 (2004) 4061.
[2] V. G. Wizer, H.W. Brandhorst, J. D. Broder, R.E.Hart, J. H. Lamneck, J. Appl. Phys. 50 (6) (1979) 4443.
[3] S.W. Glunz, S. Rein, J.Y. Lee, W. Warta, Journal of Applied Physics 90 (2001) 2397.
[4] L. Ventura, A. Slaoui, J. C. Muller, Proceedings of the 13th European Photovoltaic Solar Energy Conference, (1995) 1578-1571.
[5] U. Jäger, M. Okanovic, M. Hörteis, A. Grohe, R. Preu, Proceedings of the 24th European Photovoltaic Solar Energy Conference, (2009) 1740-1743.
[6] T. Röder, S. Eisele, P. Grabitz, C. Wagner, G. Kulushich, J. R. Köhler, J. H. Werner, Prog. Photovolt: Res. Appl., 18 (2010) 505-510.
[7] W. Shockley, Technical Report No. AL-TDR-64-207, Ohio: Air Force Atomic Laboratory, Air Force Systems Command, Wright-Patterson Air Force Base (1964).
[8] H. Berger, Journal of the Electrochemical Society 119 (1972) 507-14.
[9] H. Berger, IEEE International Solid-State Circuits Conference XII (1969) 160-161.
[10] H. Murrmann, D. Widmann, IEEE Trans. Electron Devices 16 (1969) 1022-4.
[11] P. Blood, Semicond. Sci.Technol. 1 (1986) 7–27.
[12] R. Kitamura, L. Pilon, M. Jonasz, Applied Optics 46, No. 33 (2007).
[13] M. von Arx, O. Paul, H. Baltes, Journal of Microelectromechanical Systems 9(1) (2000) 136-145.
[14] J. Kirchhof, S. Unger, J. Dellith, A. Scheffel, C. Teichmann, Optical Materials Express 2(5) (2012) 534-547.
[15] H. Kodera, Jpn. J. Appl. Phys. 2 (1963) 212-219.
[16] U. Jaeger, A. Wolf, B. Steinhauser, J. Benick, J. Nekarda, R. Preu, SPIE 8473, (2012) 847309-847309.
[17] A. S. Grove, O. Leistiko, C. T. Sah, J. Appl. Phys. 35 (1964) 2695.
[18] K. Hoh, H. Koyama, K. Uda, Y. Miura, Jap. J. Appl. Phys 19, L375 (1980).
[19] M. F. Ametowobla, PhD thesis, Institut für Physikalische Elektronik der Universitat, Stuttgart, (2010).
[20] D.E. Kane, R.M. Swanson, Proceedings of the 18th IEEE Photovoltaic Specialists Conference (1985) 1761.
[21] M. J. Kerr, A. Cuevas, J. Appl. Phs. 91 (4) (2002) 2473.
[22] P. Saint-Cast, A. Richter, E. Billot, M. Hofmann, J. Benick, J. Rentsch, R. Preu, S. W. Glunz, Thin Solid Films 522 (2012) 336-339.
[23] S. Fritz, S. Riegel, S. Gloeger, D. Kohler, M. König, M. Härtheis, G. Hahn, Proceedings of the 3rd Internation Conference on Crystalline Silicon Photovoltaics (Silicon PV), Energy Procedia 38 (2013) 720-724.